eRF3b-37 inhibits the TGF-β1-induced activation of hepatic stellate cells by regulating cell proliferation, G_0/G_1 arrest, apoptosis and migration

ZHENGRONG XU[1,2], TAO LI[1], MAN LI[1], LEI YANG[1], RUDAN XIAO[1], LI LIU[1], XIN CHI[1] and DIANWU LIU[1]

[1]Department of Epidemiology, Hebei Medical University, Shijiazhuang, Hebei 050017;
[2]Department of Preventive Medicine, Hebei North University, Zhangjiakou, Hebei 075000, P.R. China

Received January 23, 2018; Accepted September 20, 2018

DOI: 10.3892/ijmm.2018.3900

Abstract. The therapeutic management of liver fibrosis remains an unresolved clinical problem. The activation of hepatic stellate cells (HSCs) serves a pivotal role in the formation of liver fibrosis. In our previous study, matrix-assisted laser desorption/ionization time-of-flight mass spectrometry (MALDI-TOF MS) was employed to identify potential serum markers for liver cirrhosis, such as eukaryotic peptide chain releasing factor 3b polypeptide (eRF3b-37), which was initially confirmed by our group to serve a protective role in liver tissues in a C-C motif chemokine ligand 4-induced liver cirrhosis mouse model. Therefore, eRF3b-37 was hypothesized to affect the activation state of HSCs, which was determined by the expression of pro-fibrogenic associated factors in HSCs. In the present study, peptide synthesis technology was employed to elucidate the role of eRF3b-37 in the expression of pro-fibrogenic factors induced by transforming growth factor-β1 (TGF-β1) in LX-2 cells that were treated with either control, TGF-β1 and TGF-β1+eRF3b-37. 3-(4,5-Dimethyl-2-thiazolyl)-2,5-diphenyltetrazolium bromide and flow cytometric assays, and fluorescent microscope examinations were performed to evaluate the effects of eRF3b-37 on proliferation viability, G_0/G_1 arrest, apoptosis and cell migration. The results of the present study indicated that eRF3b-37 inhibited the activation of HSCs. The increased mRNA and protein expression of the pro-fibrogenic factors collagen I, connective tissue growth factor and α-smooth muscle actin (SMA) stimulated by TGF-β1 were reduced by eRF3b-37 via the following mechanisms: i) Inhibiting LX-2 cell proliferation, leading to G_0/G_1 cell cycle arrest and inhibition of DNA synthesis by downregulating the mRNA expressions of Cyclin D1 and cyclin dependent kinase-4, and upregulating the levels of P21; ii) increasing cell apoptosis by upregulating the mRNA level of B-cell lymphoma-2 (Bcl-2)-associated X protein (Bax) and Fas, and downregulating the expression of Bcl-2; and iii) reducing cell migration by downregulating the mRNA and protein expression of α-SMA. In addition, eRF3b-37 is thought to serve a role in HSCs by inhibiting TGF-β signaling. Therefore, eRF3b-37 may be a novel therapeutic agent for targeting HSCs for hepatic fibrosis.

Correspondence to: Professor Dianwu Liu, Department of Epidemiology, Hebei Medical University, 361 Zhong-shan East Road, Shijiazhuang, Hebei 050017, P.R. China
E-mail: dwliu1956@hotmail.com

Key words: eukaryotic peptide chain release factor guanosine triphosphate-binding subunit, transforming growth factor-β, hepatic stellate cell, hepatic fibrosis, collagen, liver, proliferation, apoptosis, migration

Introduction

The development of liver fibrosis is known to ultimately led to liver cirrhosis (LC). It is characterized by the excessive accumulation of extracellular matrix (ECM) and activated hepatic stellate cells (HSCs) undergo myofibroblast transition, which is identified by α-smooth muscle actin (α-SMA) expression (1). Currently there are no reliable, cost-effective and noninvasive measures available to treat LC (2). To date, the exploratory therapy used to treat hepatic fibrosis is the removal or reduction of scar accumulation in experimental models of chronic liver injury. Clinical trials evaluating the safety and efficacy of some of these treatments are anticipated in the coming years.

HSCs are the primary targets of fibrogenic stimuli in the damaged liver, and are known to be involved in the pathogenesis of many types of liver disease, particularly in fibrosis and ECM remodeling for which its key role is well established. When the liver becomes inflamed or injured by mechanical stimulation, HSCs rich in retinol are activated and migrate to the liver injury site (3,4). On the one hand, the number of activated HSCs increase in the injured site through paracrine and autocrine effects; however, on the other hand, these activated HSCs, which assume a myofibroblast-like phenotype, also transform into muscle fibrotic cells through morphological and functional changes, which then migrate and proliferate at the sites of liver injury, perpetuating hepatic inflammation and increasing the formation of stress fibers and the accumulation of α-SMA (3,5-7). A large amount of ECM is then synthesized, secreted and not degraded, ultimately depositing in the

liver. Therefore, activated HSCs are considered to be major cellular targets in the prevention of the progression of liver fibrosis. In fact, the majority antifibrotic treatments that are currently under evaluation have aimed to inhibit the activation, proliferation or synthetic products of HSCs (3). The identification of key cytokines involved in the accumulation process of activated HSCs in chronic liver diseases and the elucidation of the molecular mechanisms responsible for increased ECM levels have led to the development of pathophysiologically based strategies to treat liver fibrosis (7). Therefore, the search and development of reliable antifibrotic strategies targeting HSCs that can prevent, inhibit or reverse hepatic fibrosis by influencing the expression of pro-fibrogenic factors is urgently required.

Transforming growth factor-β1 (TGF-β1), a key inflammatory and fibrogenic peptide growth factor, has complex biological effects on cells and is a key mediator in the development of liver fibrosis. TGF-β1 has been shown to be involved in the activation of HSCs and/or has high expression during liver fibrogenesis (8). TGF-β1 can activate fibroblast cells and HSCs, and promote the cell synthesis of matrix proteins, including fibronectin, and type I, III and IV collagen; it also prevents the degradation of ECM, leading to a large number of extracellular ECM deposits, which eventually form hepatic fibrosis (1,9). In addition, it is also a multifunctional cytokine that serves various roles in wound healing, chemotaxis, mitogenesis, apoptosis, migration, differentiation, ECM synthesis and immunomodulation (9). In experimental disease models, the inhibition of the TGF-β signaling pathway, which is activated in response to liver injury, is closely associated with the subsequent onset of fibrogenesis (10,11).

In our previous study, weak cation-exchange magnetic bead purification and matrix-assisted laser desorption/ionization time-of-flight mass spectrometry (MALDI-TOF MS) was used to identify potential serum markers for LC in protein expression profiles. A 4,210 Da protein, coded for by the G_1 to S phase transition 2 (GSPT2) gene, was expressed differently between the LC, hepatocellular carcinoma (HCC) and chronic hepatitis B groups, but showed no significant difference between the HCC and LC groups (12). It was later identified as a eukaryotic peptide chain release factor guanosine triphosphate-binding subunit known as eukaryotic release factor (eRF), a part of the eRF3b lysate, including 37 amino acids (eRF3b-37). eRF3b-37 may be involved in the progression of liver fibrotic diseases, such as LC, which forms as a result of liver fibrosis.

In order to clarify the role of eRF3b-37 in the occurrence and development of liver fibrotic disease, the present study investigated its effect on the activation state of HSCs, which was determined by the expression of pro-fibrogenic factors induced by TGF-β1 in LX-2 cells and its mechanism concerning HSC proliferation, DNA synthesis, cell apoptosis and migration by polypeptide synthesis technology *in vitro*.

Materials and methods

Chemicals. Recombinant human TGF-β1 protein (PeproTech, Inc., Rocky Hill, NJ, USA) was used to stimulate LX-2 cells. The eRF3b-37 was synthesized by purification with high performance liquid chromatography (HPLC) and identification via mass spectrometry, which was performed by Sangon Biotech Co., Ltd. (Shanghai, China). The primary antibodies used were as follows: TGF-β1 (cat. no. gtx110630), collagen I (ColI; cat. no. gtx20292), connective tissue growth factor (CTGF; cat. no. gtx124232), α-smooth muscle actin (SMA; cat. no. gtx100034) and glyceraldehyde-3-phosphate dehydrogenase (GAPDH; cat. no. gtx100118) were purchased from GeneTex, Inc. (Irvine, CA, USA). The anti-eRF3b antibody against human eRF3b was purchased from ProteinTech Group, Inc. (Chicago, IL, USA; cat. no. 12989-1-AP). Primers for Col1A1, CTGF, α-SMA, Cyclin D1, Cyclin-dependent kinase 4 (CDK4), P21, B-cell lymphoma 2 (Bcl-2), Bcl-2-associated X (Bax) and Fas mRNA were synthesized by Beijing Huada Genomics Research Center Co., Ltd. (Beijing, China).

Cell culture. The LX-2 cell line was a gift from Professor Sun Dianxing (Bethune International Peace Hospital, Shijiazhuang, China). LX-2 cells were grown in Dulbecco's modified Eagle's medium (DMEM; cat. no. 11965-092; Invitrogen; Thermo Fisher Scientific, Inc., Waltham, MA, USA) with 10% (v/v) fetal bovine serum (FBS; cat. no. 10099141; Invitrogen: Thermo Fisher Scientific, Inc.) supplemented with 1% penicillin and streptomycin, and incubated at 37˚C and 5% CO_2. The cells were sub-cultured upon reaching 70% confluence every 3 days.

Establishment of the TGF-β1 cell model and experimental grouping. LX-2 cells during the exponential growth period following 0.25% trypsin digestion at 37˚C for 1 min were seeded into 96-well plates at a cell density of $5.0x10^4$/ml, 100 μl/well, for 12 h at 37˚C and were made quiescent by incubating in medium containing 0.5% FBS (Invitrogen; Thermo Fisher Scientific, Inc.) at 37˚C for 12 h. Cells were then treated with TGF-β1 or eRF3b-37 at different concentrations (0.1, 1, 10, 50, 100 or 500 ng/ml) at 37˚C for 24 and 48 h, respectively. A 3-(4,5-dimethyl-2-thiazolyl)-2,5-diphenyltetrazolium bromide (MTT) assay was employed to obtain the optimum concentration of TGF-β1/eRF3b-37. The experiments were repeated six times per concentration. Following this, a TGF-β1-induced LX-2 cell model was established using the optimum concentration of TGF-β1 to observe the inhibitory effect of eRF3b-37 on hepatic pro-fibrogenic factors. LX-2 cells were divided into three groups with triplicate dishes per group: Control, TGF and TGF+eRF3b. In the TGF group, the cells were treated with 10 ng/ml TGF-β1 following starvation with serum-free DMEM. In the TGF+eRF3b group, the cells were treated with 10 ng/ml TGF-β1 fat 37˚C or 1 h following starvation, and then with 100 ng/ml eRF3b-37 at 37˚C for 24 and 48 h. Cells incubated under the same culture conditions but without stimulation served as the controls.

Cell proliferation assay. Cell proliferation was determined using the MTT method. Following cell starvation, as aforementioned, LX-2 cells were treated with TGF-β1 or TGF-β-eRF3b as aforementioned. At the designated time (24 or 48 h), 20 μl MTT (5 mg/ml) was added to each well. The medium was removed 4 h later, then 150 μl DMSO was added to dissolve the dye for 10 min. The absorbance of each well was read at 490 nm by a Biotek Microplate Reader (BioTek Instruments, Inc.,

Winooski, VT, USA). The experiments were performed six times per concentration, and the following were applied:

$$\text{Proliferation vitality (PV; \%)} = (A490_{\text{experimental group}}/A490_{\text{control group}}\text{-}1) \times 100$$

$$\text{Inhibition rate (IR; \%)} = (1\text{-}A490_{\text{experimental group}}/A490_{\text{control group}}) \times 100$$

Detection of the cell cycle and apoptosis. The cell cycle and apoptosis were detected by flow cytometry (FCM). LX-2 cells in the exponential growth period were seeded into 6-well culture plates at a density of $5x10^4$/ml and made quiescent as aforementioned. Following 24 or 48 h treatment with TGF-β1 or TGF-β1 combined with eRF3b-37, respectively, the cells were digested with 0.25% trypsin at 37˚C for 1 min and collected by centrifugation at 110 x g and 37˚C for 5 min. Cells were washed twice with cooled, sterile phosphate buffer saline (PBS) and fixed with 500 µl ice-cold 70% ethanol per 10^5 cells at 4˚C for 24 h. Cells were resuspended in a staining solution containing DNase-free RNase (100 µg/ml) and propidium iodide (50 µg/ml) was added at a final concentration of 0.05 mg/ml at 4˚C for 30 min in the dark and subjected to cell cycle and apoptosis analysis using an Epics XL flow cytometer (Beckman Coulter, Inc., Brea, CA, USA) with MultiCycle AV version 3.0 software (Innovative Cell Technologies, Inc., San Diego, CA, USA) for cell cycle analysis and EXPO™ 32 ADC version 1.1C software (Beckman Coulter, Inc.) for apoptosis analysis. The cell proliferating index (PI) was calculated according to the cell cycles as follows: $PI=[(S+G_2/M)/(G_0/G_1+S+G_2/M)] \times 100\%$.

Cell migration viability assay. Cell migrating viability was observed and migrating distances were measured under a fluorescent microscope. LX-2 cells were seeded and treated as aforementioned. The migrating distances of cells (D) in the scratched band were obtained by scratching the bottom of the dishes with a sterile tip. The cells were then measured under a fluorescent microscope at 0, 24 and 48 h following the interventions with TGF-β1 or TGF-β1 combined with eRF3b-37. The experiments were performed in triplicate in each group. The formula used for calculating the relative migrating distance was as follows: Relative Migrating Distance=[(D0-D24/48)/D0] x100%.

Whole cell extracts and reverse transcription-quantitative polymerase chain reaction (RT-qPCR). RT-qPCR was performed to detect the gene expressions of pro-fibrogenic factors in cell proliferation, migration, apoptosis and the cell cycle. LX-2 cells were seeded and the three groups were treated as aforementioned. Subsequently, total RNA was extracted at 24 h post-treatment using a total RNA isolation kit (Beijing Solarbio Science & Technology Co., Ltd., Beijing, China).

First strand cDNA was synthesized with the Thermo Scientific RevertAid First Strand cDNA Synthesis kit (Thermo Fisher Scientific, Inc.) and the 2720 Thermal Cycler (Bio-Rad Laboratories, Inc., Hercules, CA, USA). RT-PCR was performed in a 20 µl reaction mixture containing 1 µl Random Primer, 1 µl RevertAid M-MuLV Reverse Transcriptase (200 U/µl), 2 µl 10 nM dNTP Mix and 1 µl RiboLock RNase Inhibitor (20 U/µl). RT-PCR was performed with the following temperature protocol: 25˚C for 5 min, 42˚C for 60 min and 70˚C for 5 min. RT-qPCR quantification was performed using the SYBR-Green Real-Time kit (Beijing Transgen Biotech Co., Ltd., Beijing, China) and the SYBR-Green and Real-Time Rotor-Gene™ 6000 cycler (Corbett Life Science; Qiagen, Inc., Valencia, CA, USA). The primers used are listed in Table I. The 20 µl reaction mix contained: 1 µl cDNA, 0.5 µl of each primer and 10 µl 2X SYBR Master Mix. RT-qPCR was performed with the following thermal cycling conditions: 94˚C for 30 sec followed by 40 cycles of 94˚C for 5 sec, 58-60˚C for 15 sec and 72˚C for 10 sec. Experiments for each gene were repeated three times. Relative gene quantities were obtained using the $2^{-\Delta\Delta Cq}$ method (13) with GAPDH as an internal reference.

Protein expression determination. Western blotting was performed to detect pro-fibrogenic factor expression. Following treatment for 48 h, LX-2 cells were lysed in Radioimmunoprecipitation assay buffer, and protein concentration was determined using BCA protein assay kits (both from Beijing Solarbio Science & Technology Co., Ltd.). The protein solution was denatured with an equal volume of 2X SDS loading buffer for 5 min, then an equal quantity of protein (20 µg/lane) was separated by 12% SDS-PAGE and electro-transferred onto polyvinylidene difluoride membranes. Following blocking with 5% skimmed milk in PBS at 4˚C overnight, the blots were incubated with the following specific primary antibodies: TGF-β1 (1:1,000), ColI (1:1,000), CTGF (1:5,000), α-SMA (1:1,000), GAPDH (1:10,000) and GSPT2 (1:2,000) overnight at 4˚C, followed by incubation with a DyLight™ 800-conjugated goat anti-rabbit immunoglobulin G (H&L) secondary antibody (Rockland Immunochemicals Inc., Pottstown, PA, USA) diluted in 1% bovine serum albumin-PBS (cat. no. A604481; Sangon Biotech Co. Ltd.) at room temperature for 2 h in the dark. The band intensity on the membrane was measured using an Odyssey Infrared Laser Imaging System) with Odyssey version 3.0 software (LI-COR Biosciences, Lincoln, NE, USA), and GAPDH was used as an internal control.

Statistical analysis. Values are expressed as the mean ± standard deviation from duplicate samples. The differences among means of >3 groups were tested by one-way analysis of variance followed by the least significant difference post hoc test. The associations between two indices were evaluated by correlation analysis. SPSS 17.0 software (SPSS, Inc., Chicago, IL, USA) was used for statistical analysis. $P<0.05$ was considered to indicate a statistically significant difference.

Results

Validation of the eRF3b-37 sequence and determination of the optimum dosage of TGF-β1 and eRF3b-37 for LX-2 cells. The amino acid sequence of eRF3b-37 in the NCBI BLAST protein database (blast.ncbi.nlm.nih.gov/Blast.cgi?PAGE=Proteins) is KEQSD FCPWY TGLPF IPYLD NLPNF NRSID GPIRL P (Locus no. IPI00642097 GSPT2; Fig. 1A).

The eRF3b-37 mass spectrogram is presented in Fig. 1B. The charge-mass ratio was 876.05 at the highest peak in the mass spectrogram and 1,085.25 at the second highest peak.

Table I. Primer sequences for reverse transcription-quantitative polymerase chain reaction.

Gene	Primer sequences (5'-3')	Fragment length (bp)
GAPDH	Forward: TGGTATCGTGGAAGGACTCA	325
	Reverse: CCAGTAGAGGCAGGGATGAT	
GSPT2	Forward: GGAGATCCGCTCACACACAA	230
	Reverse: TCCATGGTCTCGGAACTTGC	
TGF-β1	Forward: ACAGCAACAATTCCTGGCGATAC	140
	Reverse: GCTAAGGCGAAAGCCCTCAAT	
Col1A1	Forward: CCCAGCCACAAAGAGTCTACAT	183
	Reverse: TCATGGTACCTGAGGCCGTT	
CTGF	Forward: CAACTATGATGCGAGCCAACTG	286
	Reverse: CACACCCCACAGAACTTAGCC	
α-SMA	Forward: ATCAAGGCCCAAGAAAAGCAAG	241
	Reverse: CCTCTTCTTCACACATAGCTGG	
Cyclin D1	Forward: CCCGATGCCAACCTCCTCAA	184
	Reverse: GGAAGACCTCCTCCTCGCAC	
CDK4	Forward: TCTGGTGACAAGTGGTGGAAC	228
	Reverse: TGGTCGGCTTCAGAGTTTCC	
P21	Forward: CAGGAGACCTCTAAAGACCCCA	179
	Reverse: GAATACTCCCCACATAGCCCG	
Bcl-2	Forward: GAACTGGGGGAGGATTGTGG	183
	Reverse: CCGTACAGTTCCACAAAGGC	
Bax	Forward: CGGGTTGTCGCCCTTTTCTA	105
	Reverse: GAAGTCCAATGTCCAGCCCA	
Fas	Forward: GCATCTGGACCCTCCTACCT	186
	Reverse: GAGGACAGGGCTTATGGCAG	

GAPDH, Glyceraldehyde-3-phosphate dehydrogenase; GSPT2, G_1 to S phase transition 2; TGF, transforming growth factor; Col1A1, Collagen type I α1 chain; CTGF, connective tissue growth factor; SMA, smooth muscle actin; CDK, Cyclin dependent kinase; Bcl-2, B-cell lymphoma-2; Bax, Bcl-2-associated X protein.

According to the formula: Charge-mass ratio=(Molecular weight+Charge quality)/Charge number, the molecular weight was calculated as 4,337.25 and 4,337.00 at the two peaks, respectively. Their errors were 0.006 and 0.000%, respectively, which were within the 1% normal range in the experimental study when compared with the real molecular weight 4,337. The peak figure of eRF3b-37 was specific and obtained by HPLC. The peak area was 9,202,916.00 and the eRF3b-37 concentration was 98.27% (Fig. 1C).

In order to identify the optimum dosage of TGF-β1 and eRF3b-37, the present study determined the cell proliferation activity with and without TGF-β1 and eRF3b-37 treatment. Proliferation measured at A490 and the proliferation viability of LX-2 cells treated with TGF-β1 at 0, 0.1, 1, 10, 50, 100 or 500 ng/ml at 24 and 48 h reached the highest point at 10 ng/ml (Fig. 1D and E). Proliferation measured at A490 and the inhibition rate of LX-2 cells by eRF3b-37 at 0, 0.1, 1, 10, 50, 100 or 500 ng/ml at 12, 24, 36 and 48 h were inhibited with a minimum of 100 ng/ml (Fig. 1F and G). The dose of eRF3b-37 was positively correlated with the cell inhibition rate in the concentration range of 0.1-100 ng/ml at all 4 time-points; the absolute values of Pearson correlation coefficient were 0.926, 0.992, 0.946 and 0.968, respectively. Within the range of 0.1-100 ng/ml, the inhibition of LX-2 cells by eRF3b-37 was dose-dependent. The results indicated that eRF3b-37 was of high purity, satisfying the requirement of experimental research. Therefore, TGF-β1 and eRF3b-37 acted on LX-2 with optimum concentrations of 10 and 100 ng/ml, respectively.

eRF3b-37 promotes GSPT2 and inhibits the TGF-β1 expression induced by TGF-β1 in LX-2 cells. In order to determine whether eRF3b-37 influences the expression of GSPT2 and TGF-β1, the cells were divided into three groups: Control, TGF (10 ng/ml) and TGF (10 ng/ml)+eRF3b (100 ng/ml). In regard to GSPT2, the mRNA and protein expressions of the TGF group were lower than those observed in the control or TGF+eRF3b groups at 24 and 48 h following treatment (Fig. 2A and C). With respect to TGF-β1, the mRNA and protein expressions in the TGF group were markedly higher when compared with the control and TGF+eRF3b groups (Fig. 2B and D). The results revealed that eRF3b-37 treatment increased GSPT2 expression and inhibited TGF-β1 expression. It is thought that eRF3b-37 may exert its effects on LX-2 by inhibiting TGF-β signaling. Thus, TGF-β1 was successfully used to activate HSCs and construct a fibrogenic expression model of HSCs.

eRF3b-37 decreases the mRNA and protein expression of pro-fibrogenic factors induced by TGF-β1 in LX-2 cells.

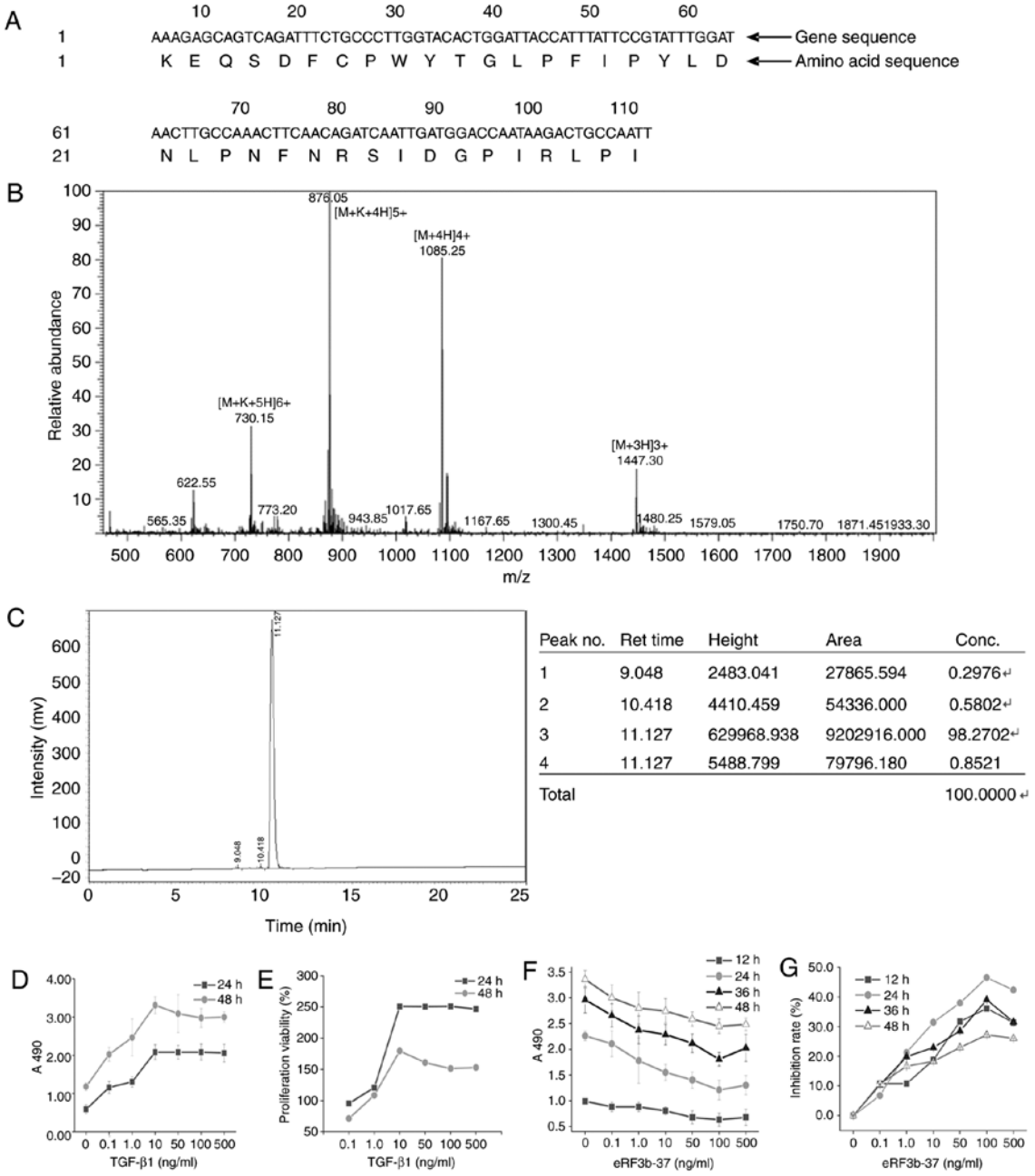

Figure 1. Validation of eRF3b-37 sequences and determination of the optimum dosage of TGF-β1 and eRF3b-37 for LX-2. (A) Nucleotide sequences and the corresponding amino acid alignments of the eRF3b-37 in *Homo* species were obtained from the NCBI BLAST protein database. eRF3b-37 identified by (B) mass-spectrogram and (C) liquid chromatogram satisfied the requirements of the experiment. (D) The A490 and (E) proliferation viability of LX-2 cells were determined by MTT following stimulation with 0, 0.1, 1, 10, 100 or 500 ng/ml TGF-β1: It reached the plating point at 10 ng/ml at 24 and 48 h. LX-2 cells were stimulated with 0, 0.1, 1, 10, 100 or 500 ng/ml eRF3b-37, and the (F) cell proliferation A490 and (G) inhibition rate reached the optimal level at 100 ng/ml at 12, 24, 36 and 48 h, as determined by MTT. Data are presented as the mean ± standard deviation of six independent repeated experiments per group. TGF, transforming growth factor; eRF3b, eukaryotic peptide chain releasing factor 3b polypeptide; MTT, 3-(4,5-dimethyl-2-thiazolyl)-2,5-diphenyltetrazolium bromide.

To evaluate the effects of eRF3b-37 on HSC activation, the mRNA and protein expression levels of pro-fibrogenic factors induced by TGF-β1 in LX-2 cells were determined. The mRNA and protein expressions of ColI, CTGF and α-SMA in the TGF group were greater than those observed in the control or TGF+eRF3b groups (Fig. 3A-F). In addition, the protein expression of GSPT2 increased, while that of α-SMA decreased with the increased dosage of eRF3b-37 (Fig. 3G). A negative correlation was also observed between GSPT2 and α-SMA expression, with a Pearson's correlation coefficient of -0.991 (Fig. 3H). The results revealed that HSC activation occurred as the TGF-β1-induced increased expression of ColI, CTGF and α-SMA by was inhibited by eRF3b-37 application; eRF3b-37 increased GSPT2 expression and inhibited α-SMA expression dose-dependently in LX-2 cells.

eRF3b-37 inhibits proliferation, promotes the G_0/G_1 arrest of the cell cycle and affects proliferative factor expression in LX-2 cells stimulated with TGF-β1. To determine the effects of eRF3b-37 on cell proliferation and the cell cycle when induced by TGF-β1, HSCs were divided into five experimental groups: Control, TGF, TGF+1.0 ng/ml eRF3b-37, TGF+10 ng/ml

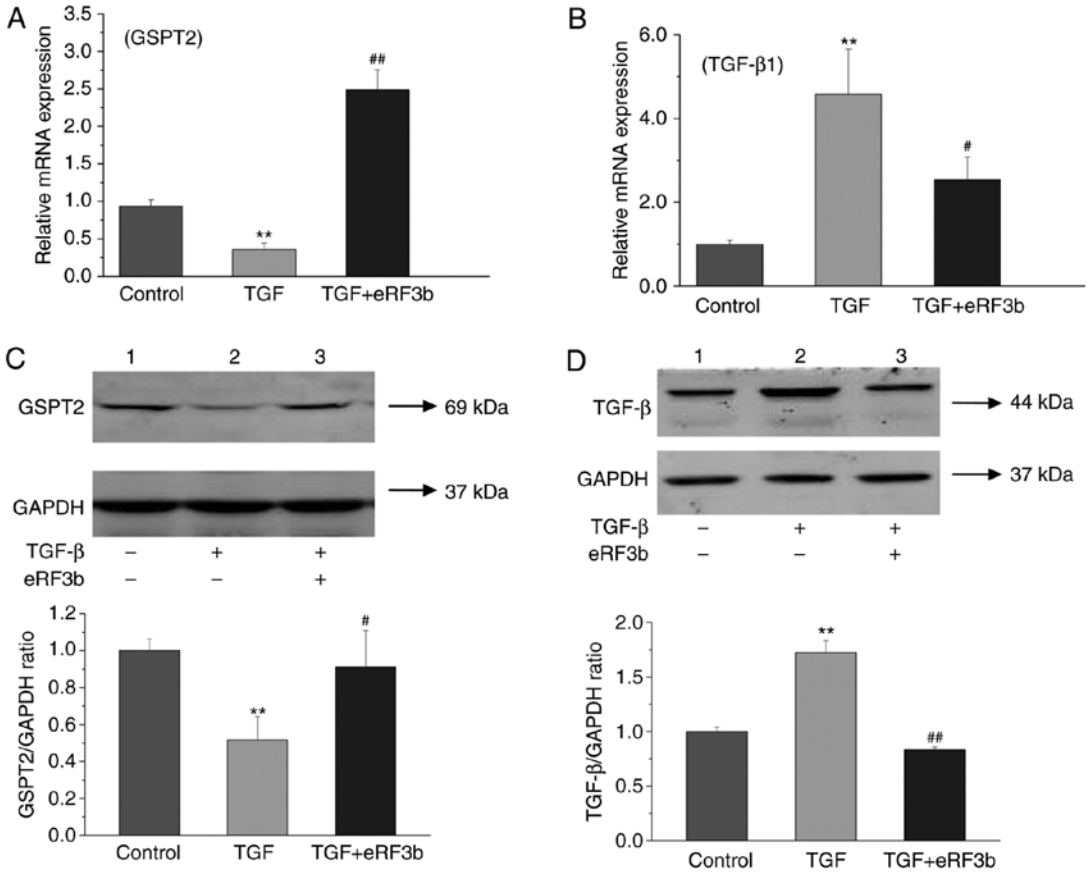

Figure 2. eRF3b-37 affects the mRNA and protein expression of GSPT2 and TGF-β1 in LX-2 cells. eRF3b-37 (A) promotes GSPT2 and (B) inhibits TGF-β1 mRNA expression as determined by reverse transcription-quantitative polymerase chain reaction at 24 h. eRF3b-37 (C) promotes GSPT2 and (D) inhibits TGF-β1 protein expression as determined by western blotting at 48 h. Data are presented as the mean ± standard deviation of three independent repeated experiments per group. **P<0.01 vs. Control group; $^{\#}$P<0.05 and $^{\#\#}$P<0.01 vs. TGF group. eRF3b, eukaryotic peptide chain releasing factor 3b polypeptide; TGF, transforming growth factor; GSPT2, G_1 to S phase transition 2.

eRF3b-37 and TGF+100 ng/ml eRF3b-37. eRF3b-37 inhibited LX-2 cell proliferation when stimulated with TGF-β1, with inhibition rates of 34.80 and 19.90% at 24 and 48 h, respectively, for the TGF+100 ng/ml eRF3b-37 group (Fig. 4A). Subsequently, the cells were divided into three groups as aforementioned. In the TGF group, there were fewer G_0/G_1 phase cells, while the number of S cells increased when compared with the control group. In the TGF+eRF3b group, the number of G_0/G_1 phase cells increased, while the number of S phase cells decreased in the TGF group; the number of G_2/M phase cells did not change significantly at 48 h (Fig. 4B-D). The PI of the TGF group was greater than that observed in control or TGF+eRF3b groups at 48 h (Fig. 4E). Cyclin D1, CDK4 and P21 are factors that regulate proliferation and cell cycle (14). The mRNA expressions of Cyclin D1 and CDK4 in the TGF group increased when compared with the control and TGF+eRF3b groups. However, the mRNA expression of P21 in the TGF group was reduced when compared the control or TGF+eRF3b groups (Fig. 4F-H). These results revealed that eRF3b-37 may inhibit cell proliferation viability, promote G_0/G_1 arrest and block DNA synthesis by downregulating the expression of Cyclin D1 and CDK4 and upregulating the level of P21 in LX-2 cells stimulated with TGF-β1.

eRF3b-37 reverses cell apoptosis and decreases cell migration viability by regulating the expression of related factors in LX-2 cells stimulated with TGF-β1. At 48 h, the apoptotic rate of HSCs was lower in the TGF group than in the control group; however, no statistical difference was observed as the apoptotic rate in the control group was quite low. The rate of apoptosis was significantly greater in the eRF3b group when compared with the TGF group (Fig. 5A and B). Bcl-2, Bax, and Fas are factors that regulate cell apoptosis (15,16). The mRNA expression of Bcl-2 in the TGF group was higher than that of the control and TGF+eRF3b groups. By contrast, the expressions of Bax and Fas in the TGF group were lower than those observed in the control or TGF+eRF3b groups (Fig. 5C-E).

In addition, the increase in HSC migrating activity is indicative of cell activation. The migrating distances of the three groups were observed, photographed, measured, and compared under the microscope at the same magnification and position on the scratch at 0, 24 and 48 h (Fig. 5G and H). Under the microscope, the HSC morphology in the control group was complete and orderly, and the size was uniform; however, the rate of proliferation was slow. While in the TGF group, the body of HSCs gradually increased, with cell protrusions expanding into a spindle shape; the cells grew in clusters and proliferated rapidly. The relative migrating distance was larger in the TGF group than in the control or TGF+eRF3b groups at 24 and 48 h (Fig. 5F).

The results indicated that eRF3b-37 may promote cell apoptosis by downregulating Bcl-2, and upregulating the

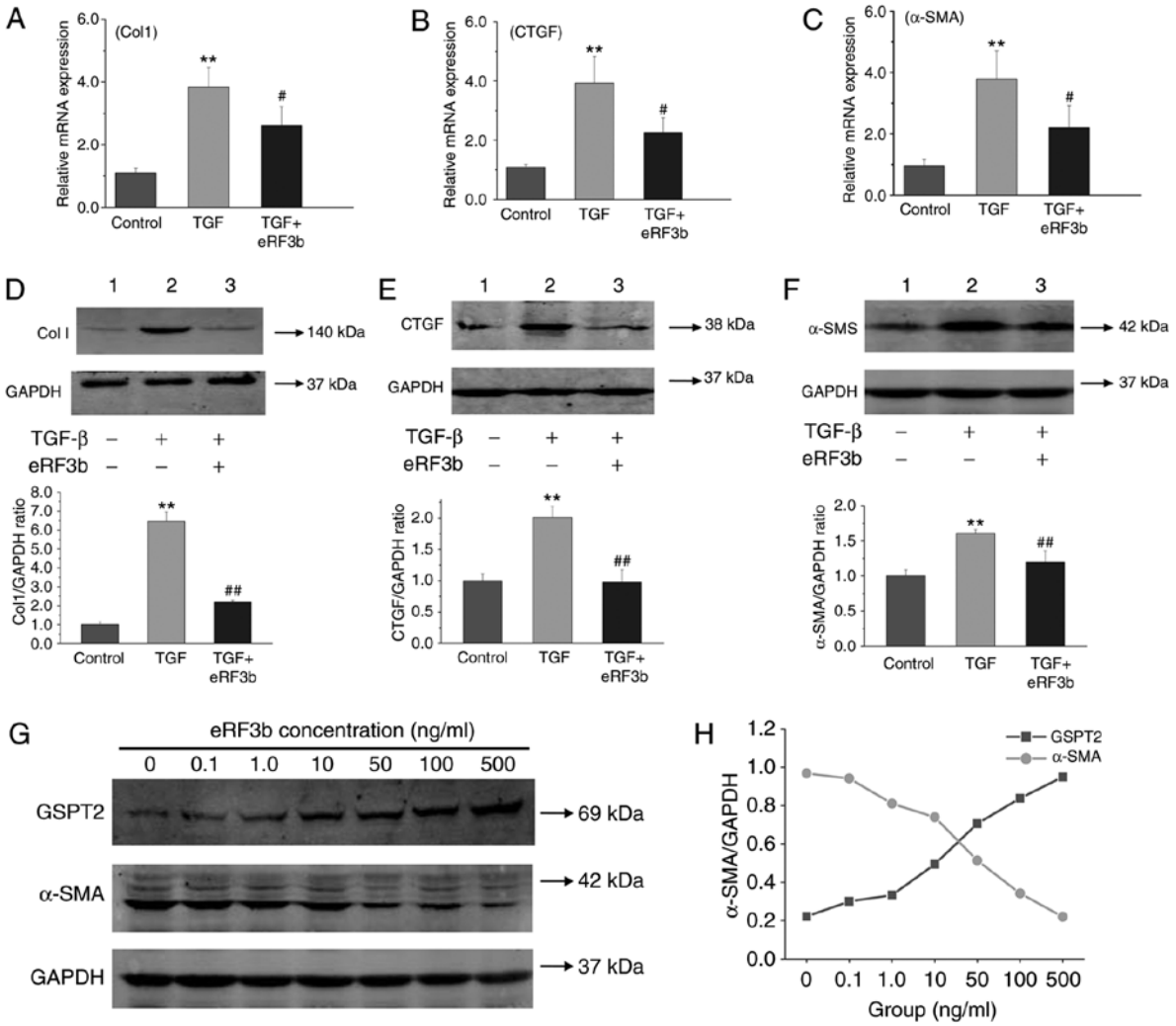

Figure 3. eRF3b-37 decreases the mRNA and protein levels of the pro-fibrotic factors ColI, CTGF and α-SMA TGF-β1-stimulated in LX-2 cells. eRF3b-37 inhibited the mRNA expression of (A) ColI, (B) CTGF and (C) α-SMA, as determined by reverse transcription-quantitative polymerase chain reaction at 24 h. eRF3b-37 inhibited the protein expression of (D) Col I, (E) CTGF and (F) α-SMA as determined by western blotting at 48 h. (G) Doses of 0.1, 1, 10, 100 or 500 ng/ml of eRF3b-37 increased GSPT2 expression and inhibited the expression of α-SMA dose-dependently at 48 h. (H) Statistical analysis indicated that there was a negative correlation between GSPT2 and α-SMA protein expression. Data are presented as the mean ± standard deviation of three independent repeated experiments per group. **P<0.01 vs. Control group; $^{\#}$P<0.05 and $^{\#\#}$P<0.01 vs. TGF group. eRF3b, eukaryotic peptide chain releasing factor 3b polypeptide; CTGF, connective tissue growth factor; SMA, smooth muscle actin; TGF, transforming growth factor; Col, collagen; GSPT2, G_1 to S phase transition 2.

expression of Bax and Fas. Furthermore, eRF3b-37 restricts cell migration abilities by decreasing α-SMA expression in LX-2 cells stimulated with TGF-β1.

Discussion

TGF-β1 is a pro-fibrotic factor involved in the fibrotic process, which induces the formation of HSC collagen through the classical TGF-β/mothers against decapentaplegic homolog and P38/mitogen-activated protein kinase signaling pathways (8,17). TGF-β1 also elevates CTGF expression and in turn, enhances the mRNA expression of ColI and III. HSCs are mesenchymal cells that respond to liver injury in a stepwise manner, thereby transitioning from quiescent, vitamin A-rich, non-proliferative cells to an activated contractile myofibroblast phenotype characterized by an increase in DNA synthesis, proliferation viability, α-SMA expression, and the synthesis of various ECM components (18,19). This activation consists of an initiation stage, a perpetuation stage and a resolution phase, where liver injury is resolved (20). Therefore, the activation of HSC, stimulated by TGF-β1, was employed as the starting point to explore the mechanism underlying the effect of eRF3b-37 on HSC activation and pro-fibrogenic-associated factor expression. TGF-β1 was used to successfully construct a HSC fibrogenic expression model with an optimal dose of 10 ng/ml, which is consistent with previous literature (21).

When the liver is injured by inflammation or mechanical stimulation, HSCs are activated, which is followed by an increase in proliferation activity and thus, the number of cells. In addition, their morphology and function also change into myofibroblast-like cells, which express α-SMA and secrete a substantial amount of collagen fibers that mainly contain type I and III (3,22). Freshly isolated quiescent HSCs synthesize minimal quantities of collagen, whereas activated HSCs express high levels of the genes encoding procollagen I and III, and secrete large amounts of collagen (6). CTGF belongs to the calponin family of proteins and is a downstream mediator of TGF-β1 (23,24). The CTGF promoter sequence contains a

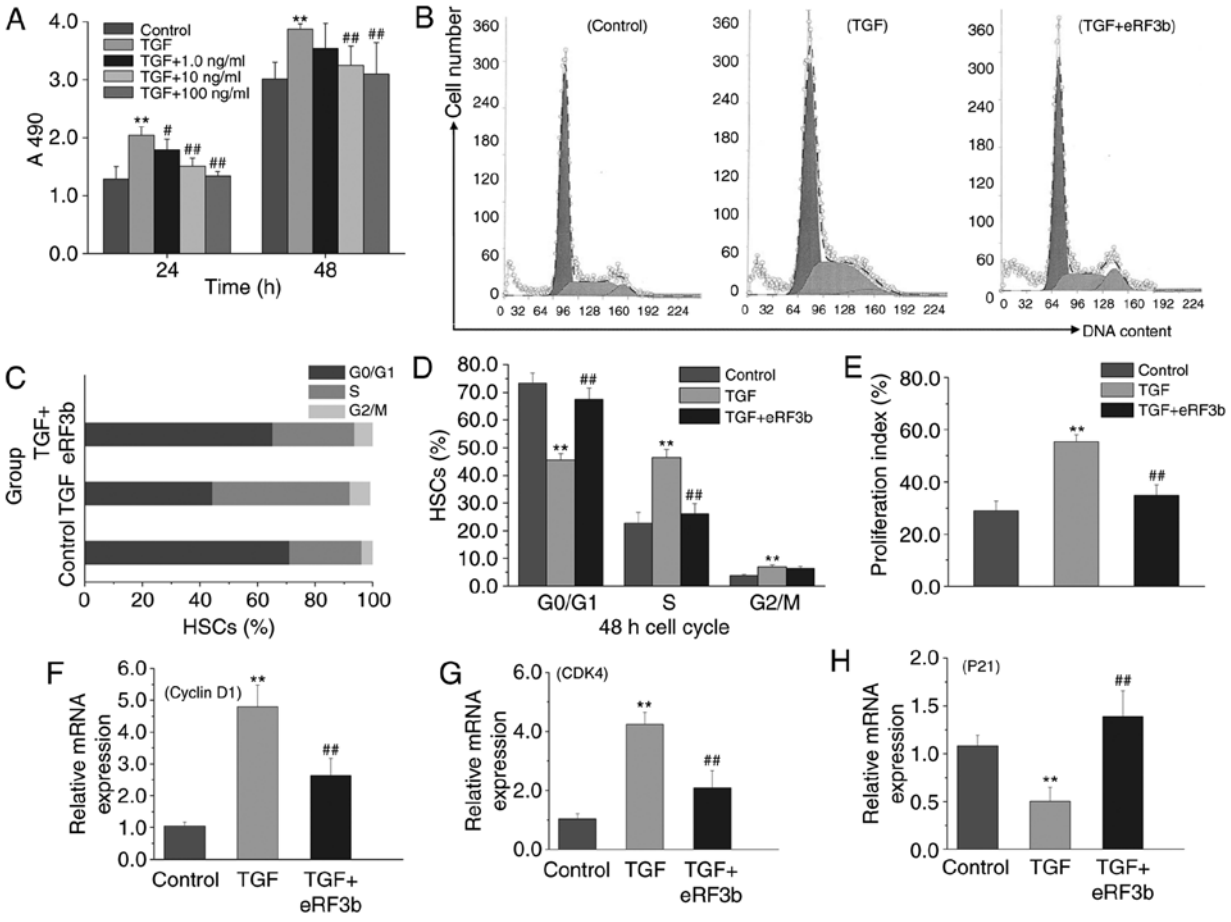

Figure 4. eRF3b-37 inhibits cell proliferation and promotes G_0/G_1 cell cycle arrest, as well as markedly affecting the expression of proliferative factors in LX-2 cells stimulated with TGF-β1. (A) eRF3b-37 inhibited LX-2 proliferation when stimulated with TGF-β1, as determined by (4,5-dimethyl-2-thiazolyl)-2,5-diphenyltetrazolium bromide assay at 24 and 48 h. (B) eRF3b-37 increased the number of G_0/G_1 phase cells and downregulated the number of S phase cells, as determined by FCM. (C) A percentage bar chart and (D) statistical analysis results presenting the effects of eRF3b-37 on the cell cycle. (E) eRF3b-37 inhibited the proliferation index (%) of HSCs stimulated with TGF-β1, as determined by FCM. eRF3b-37 regulated the mRNA expression of (F) Cyclin D1, (G) CDK4 and (H) P21, as determined by reverse transcription-quantitative polymerase chain reaction. Data are presented as the mean ± standard deviation of three independent repeated experiments per group. **P<0.01 vs. Control group; $^{\#}$P<0.05 and $^{\#\#}$P<0.01 vs. TGF group. eRF3b, eukaryotic peptide chain releasing factor 3b polypeptide; TGF, transforming growth factor; CDK, Cyclin-dependent kinase; FCM, flow cytometry; HSCs, hepatic stellate cells.

unique TGF-β response regulatory element. TGF-β1 elevated the expression of CTGF at the mRNA and protein levels in the fibrotic hypertrophy of the ligamentum flavum (25). Williams *et al* (26) reported that CTGF appears to be directly involved in HSC biology, as it is produced as a function of the activation or exposure of cells to TGF-β1. Accordingly, the results of the present study demonstrated that the increased expressions of ColI, CTGF and α-SMA reflect the pro-fibrogenic tendency of HSCs stimulated with TGF-β1. It was deduced that TGF-β1 may directly stimulate the expression of ColI, CTGF and α-SMA in HSCs, or stimulate ColI and α-SMA by activating its downstream cytokine, CTGF. The inhibitory effect of eRF3b-37 on ColI, CTGF and α-SMA expression may be attributable to the downregulation of TGF-β1. eRF3b-37 is thought to serve a role in HSC by inhibiting TGF-β signaling.

The cell cycle assay is a rapid and accurate method used to study cell proliferation. The cell cycle is the basic process of cell life that contains four phases: The G_0/G_1 phase (DNA synthesis prophase), S phase (DNA synthesis phase), G_2 phase (DNA synthesis anaphase) and M phase (DNA division phase) (14,27). The cell is prepared for DNA replication in the G_1 phase, and then chromosomes are replicated during the S phase. A gap period, G_2, allows for preparation for mitosis prior to chromosome segregation and cytokines are produced in the M phase (mitosis). G_0/G_1 is an important checkpoint; the restriction point occurs mid-G_1. Following this checkpoint, cells become independent of growth factors and commit to cell division. S phase cells participate in cell division, thereby representing the number of cells involved in the division (14,27). In fact, changes in the ratios of G_0/G_1 to S+G_2/M cells can reflect cell proliferation and cell cycle status (14). In the present study, eRF3b-37 inhibited cell proliferation, increased G_0/G_1 arrest and blocked DNA synthesis in HSCs by inhibiting TGF-β1. eRF3b-37 may have inhibited proliferation capabilities by promoting G_0/G_1 arrest and blocking DNA synthesis.

Proliferation and cell-cycle progression are regulated by two protein classes: Cyclins and their associated kinase partners, CDKs. Cyclin D is the prime integrator of these cellular signals, initiating progression through the early phase of the G_1 period (14,28). Cyclin D activity is required to regulate the progression from G_1 into the S phase partly mediated through coordinated CDK4/6-dependent phosphorylation of the retinoblastoma substrate (Rb). The regulation of Cyclin/CDK activity

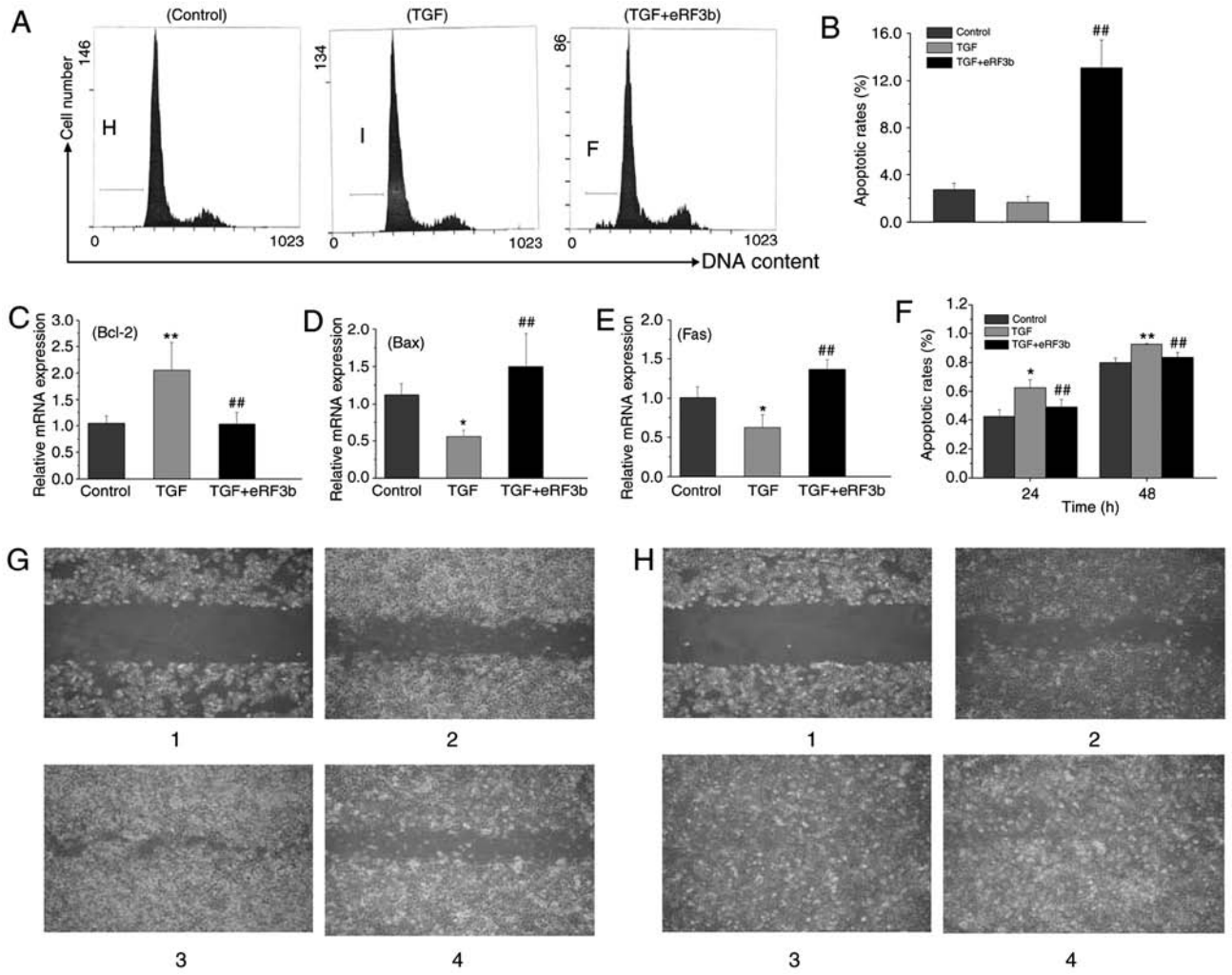

Figure 5. eRF3b-37 reverses cell apoptosis and reduces cell migration viability by regulating associated factor expression in LX-2 cells stimulated with TGF-β1. (A) eRF3b-37 reverses the cell apoptosis induced by TGF-β1, as determined by flow cytometry at 48 h. (B) Statistical analysis revealed that the apoptotic rate was higher in the TGF+eRF3b group when compared with the TGF group. eRF3b-37 regulates the mRNA expression of (C) Bcl-2, (D) Bax and (E) Fas, as determined by reverse transcription-quantitative polymerase chain reaction at 24 h. (F) Statistical analysis of the effects of eRF3b-37 on cell migration. eRF3b-37 reduced cell migration abilities at (G) 24 and (H) 48 h respectively (fluorescence microscope; magnification, x4.2). Image 1 is day 0; images 2, 3 and 4 are the control, TGF and TGF+eRF3b groups, respectively. Data are presented as the mean ± standard deviation of three independent repeated experiments per group. *P<0.05 and **P<0.01 vs. Control group; $^{\#\#}$P<0.01 vs. TGF group. eRF3b, eukaryotic peptide chain releasing factor 3b polypeptide; TGF, transforming growth factor; Bcl-2, B-cell lymphoma 2; Bax, Bcl-2-associated X protein.

is central to restriction-point passage (14). Cyclin D1 serves a more prominent role in driving cell cycle progression when in comparison with other members of the Cyclin D family. Once bound to Cyclin, CDK4 can exert its important biological role in protein kinase activity (14,29). Cyclin D1 alone has been reported to bind CDK4 and initiate the phosphorylation of Rb family proteins, which in turn, dictate the events that orchestrate mitosis; these events may regulate cell proliferation, differentiation and the cell cycle, inducing cell cycle progression from G_1 to S (14,28,30). P21 belongs to the Cip/Kip family of cell cycle inhibitors. The P21 family can interact with cyclin and CDK subunits. In the G_1/S transition phase of the cell-cycle, the negative cell-cycle regulator is responsible for suppressing Cyclin D1/CDK4 complexes (23). Qin *et al* (31) transfected the P21 gene into hepatoma Hep3B cells and revealed that the increased expression of P21 inhibited the growth of Hep3B cells. The P21 C terminal domain can directly bind to the proliferating cell nuclear antigen (PCNA), and inhibit the binding of DNA polymerase δ and PCNA in the process of G_1/S transformation, thereby blocking DNA replication in the cell cycle (32). Therefore, it could be deduced that eRF3b-37 can arrest cell proliferation, the G_0/G_1 cell cycle and DNA synthesis by inhibiting the expressions of Cyclin D1 and CDK4, and upregulating the expression of P21 induced by TGF-β1.

Apoptosis is the major pathway for the reduction of HSCs. TGF-β may decrease the spontaneous apoptosis of HSCs and support activated HSC survival by regulating Fas Ligand (FasL) synthesis and Bcl, NF-kB, and p53/$P21^{WAF1}$ signaling (15,16). The results of the present study are consistent with these previous reports. eRF3b-37 may increase the apoptosis of TGF-β1-induced LX-2 cells; however, the result does not have much practical significance due to the very low apoptotic rate of HSCs.

Many relevant factors are involved in the regulation of this apoptotic process. Previous studies have demonstrated that the regulation of apoptosis primarily depends on two conserved signaling pathways: The mitochondrial pathway and the death receptor pathway. The major regulator of the mitochondrial

apoptosis pathway, the Bcl-2 gene family, inhibits or promotes apoptosis by blocking or stimulating, respectively, the release of cytochrome C into the cytoplasm (33,34). The Bcl-2 gene family is divided into two groups: Anti-apoptotic factors, such as Bcl-2; and pro-apoptotic factors, such as Bax. The apoptosis of HSC is believed to be due to the imbalanced expression of Bcl-2 and Bax. Bcl-2 can decrease apoptosis mediated by TNF-α or the Fas system; in particular, it can change human HSC/MF sensitivity to TNF-α-induced apoptosis (35). Bax proteins induce the apoptosis of HSC by translocating directly from the cytoplasm to the mitochondria and the cytosolic liberation of cytochrome C (35-37). Bcl-2 prevents Bax from translocating from the cytosol to the mitochondria by capturing Bax monomers prior to their dimerization, thereby preventing Bax from forming channels in the mitochondrial outer membrane (38). The death receptor pathway is mediated by the death factor FasL, and its corresponding death factor receptor, Fas. Fas is located in the target cell membrane, binding to the specific ligand FasL and then initiating the apoptosis process. Saile *et al* (37) reported that the occurrence of spontaneous apoptosis in HSCs during activation was accompanied by an increased expression of Fas/FasL in HSCs. Therefore, eRF3b-37 was hypothesized to promote HSC apoptosis in association with the downregulation of Bcl-2 and the upregulation of Bax and Fas genes, when induced by TGF-β1. Consequently, eRF3b-37 may regulate cell apoptosis through the mitochondrial and death receptor pathways.

HSC directional migration and adhesion also serves important roles in an injured or inflamed liver. HSCs release many cytokines that are involved in the process of cell migration. In particular, TGF-β1 can promote the cytoskeletal remodeling and migration of HSCs by inducing the robust generation of stress fibers and focal adhesions, acquisition of spindle morphology, and increased motility (6,39). Actin is closely associated with cell migration. One component of the HSC cytoskeleton is actin filament, such as α-SMA, which provides structural support for cell migration and contraction. Actin constitutes the chemical machinery system of cell movement, using chemical energy to produce mechanical movement (40). Increased α-SMA expression in fibroblasts enhances the ability of actin to generate contractile force (41). Consequently, α-SMA acts as an indicator of HSC activation and indirectly reflects its migration capacity *in vitro*. In the present study, it was assumed that TGF-β1 induced cell migration by upregulating α-SMA expression. The inhibitory action of eRF3b-37 on HSC migration may be partly associated with the downregulation of α-SMA induced by TGF-β1.

In conclusion, eRF3b-37 inhibited the activation of HSCs and the expression of pro-fibrogenic factors in LX-2 cells stimulated with TGF-β1 by decreasing cell proliferation viability, reducing DNA synthesis and cell apoptosis arrest, and inhibiting cell migration, which are closely associated with changes in their corresponding regulatory factors in HSCs. In addition, eRF3b-37 is thought to exert its effects on HSCs by inhibiting TGF-β signaling. Consequently, the present results may contribute to the understanding of the roles of TGF-β1 and eRF3b-37 in the pathogenesis of HSCs in liver fibrosis. It should be noted that the present study only focuses on our initial work associated with the effects of eRF3b-37 on HSC and thus, one limitation was that only one cell line was used. In the future, the group will further investigate the underlying mechanism of eRF3b-37 in HSC and animal models, for example, how it works via various cytokine signal pathways and calcium ions. eRF3b-37 may be a novel therapeutic agent for targeting HSCs for hepatic fibrosis, though its mechanism still requires more in-depth study.

Acknowledgements

Not applicable.

Funding

The present study was supported by grants from the Major Projects of Hebei Province Natural Science Foundation of China (grant no. H2016206576).

Availability of data and materials

All data generated or analyzed during this study are included in this published article.

Authors' contributions

ZX drafted the manuscript and performed the major experiments. DL gave final approval of the version to be published and revised it critically for important intellectual content. TL was involved in project design, supervision and cell culture experiments. ML analyzed and interpreted the data and performed RT-qPCR. LY conducted western blotting and was involved in designing the study. RX, LL and XC were involved in the experiments. All authors read and approved the final manuscript.

Ethics approval and consent to participate

Not applicable.

Patient consent for publication

Not applicable.

Competing interests

The authors declare that they have no competing interests.

References

1. Tang LX, He RH, Yang G, Tan JJ, Zhou L, Meng XM, Huang XR and Lan HY: Asiatic acid inhibits liver fibrosis by blocking TGF-beta/Smad signaling in vivo and in vitro. PLoS One 7: e31350, 2012.
2. Gressner AM, Yagmur E, Lahme B, Gressner O and Stanzel S: Connective tissue growth factor in serum as a new candidate test for assessment of hepatic fibrosis. Clin Chem 52: 1815-1817, 2006.
3. Tsukada S, Parsons CJ and Rippe RA: Mechanisms of liver fibrosis. Clin Chim Acta 364: 33-60, 2006.
4. Zhang CY, Yuan WG, He P, Lei JH and Wang CX: Liver fibrosis and hepatic stellate cells: Etiology, pathological hallmarks and therapeutic targets. World J Gastroenterol 22: 10512-10522, 2016.
5. Peelman F, Waelput W, Iaerentant H, Lavens D, Eyckerman S, Zabeau L and Tavenier J: Leptin: Linking adipocyte metabolism with cardiovascular and autoimmune diseases. Prog Lipid Res 43: 283-301, 2004.

6. Li L, Wang JY, Yang CQ and Jiang W: Effect of RhoA on transforming growth factor β1-induced rat hepatic stellate cell migration. Liver Int 32: 1093-1102, 2012.
7. Bataller R and Brenner DA: Hepatic satellite cells as a target for the treatment of liver fibrosis. Semin Liver Dis 21: 437-451, 2001.
8. Chung YJ, Lee JI, Chong S, Seok JW, Park SJ, Jang HW, Kim SW and Chung JH: Anti-proliferative effect and action mechanism of dexamethasone in human medullary thyroid cancer cell line. Endocr Res 36: 149-157, 2011.
9. Qi W, Chen X, Poronnik P and Pollock CA: Transforming growth factor- beta/connective tissue growth factor axis in the kidney. Int J Biochem Cell Biol 40: 9-13, 2008.
10. Marquez-Aguirre A, Sandoval-Rodriguez A, Gonzalez-Cuevas J, Bueno-Topete M, Navarro-Partida J, Arellano-Olivera I, Lucano-Landeros S and Armendariz-Borunda J: Adenoviral delivery of dominant-negative transforming growth factor beta type II receptor upregulates transcriptional repressor SKI-like oncogene, decreases matrix metalloproteinase 2 in hepatic stellate cell and prevents liver fibrosis in rats. J Gene Med 11: 207-219, 2009.
11. George J, Roulot D, Koteliansky VE and Bissell DM: In vivo inhibition of rat stellate cell activation by soluble transforming growth factor beta type II receptor: A potential new therapy for hepatic fibrosis. Proc Natl Acad Sci USA 96: 12719-12724, 1999.
12. Li M, Wang J, Dai E and Liu D: Identification and investigation of disease-related peptides in sera from patients with chronic hepatitis B. Wei Sheng Yan Jiu 40: 315-319, 2011 (In Chinese).
13. Livak KJ and Schmittgen TD: Analysis of relative gene expression data using real-time quantitative PCR and the 2(-Delta Delta C(T)) method. Methods 25: 402-408, 2001.
14. Swanton C: Cell-cycle targeted therapies. Lancet Oncol 5: 27-36, 2004.
15. Saile B, Matthes N, Knittel T and Ramadori G: Transforming growth factor beta and tumor necrosis factor alpha inhibit both apoptosis and proliferation of activated rat hepatic stellate cells. Hepatology 30: 196-202, 1999.
16. Saile B, Matthes N, EI Armouche H, Neubauer K and Ramadori G: The bcl, NFkappaB and p53/p21WAF1 systems are involved in spontaneous apoptosis and in the anti-apoptotic effect of TGF-beta or TNF-alpha on activated hepatic stellate cells. Eur J Cell Biol 80: 554-561, 2001.
17. Breitkopf K, Godoy P, Ciuclan L, Singer MV and Dooley S: TGF-beta/Smad signaling in the injured liver. Z Gastroenterol 44: 57-66, 2006.
18. Gao R, Ball DK, Perbal B and Brigstock DR: Connective tissue growth factor (CCN2) induces c-fos gene activation and cell proliferation through p42/44 MAP kinase (ERK1/2) in primary rat hepatic stellate cells. J Hepatol 40: 431-438, 2004.
19. Deng ZY, Li J, Jin Y, Chen XL and Lü XW: Effect of oxymatrine on the p38 mitogen-activated protein kinases signalling pathway in rats with CCl4 induced hepatic fibrosis. Chinese Med J (Engl) 122: 1449-1454, 2009.
20. Kocabayoglu P and Friedman SL: Cellular basis of hepatic fibrosis and its role in inflammation and cancer. Front Biosci (Schol Ed) 5: 217-230, 2013.
21. Shimada H, Staten NR and Rajagopalan LE: TGF-β1 mediated activation of Rho kinase induces TGF-β2 and endothelin-1 expression in human hepatic stellate cells. J Hepatol 54: 521-528, 2011.
22. Higashi T, Friedman SL and Hoshida Y. Hepatic stellate cells as key target in liver fibrosis. Adv Drug Deliv Rev 121: 27-42, 2017.
23. Qi W, Twigg S, Chen X, Polhill TS, Poronnik P, Gilbert RE and Pollock CA: Integrated actions of transforming growth factor-beta1 and connective tissue growth factor in renal fibrosis. Am J Physiol Renal Physiol 288: F800-F809, 2005.
24. Yokoi H, Sugawara A, Mukoyama M, Mori K, Makino H, Suganami T, Nagae T, Yahata K, Fujinaga Y, Tanaka I and Nakao K: Role of connective tissue growth factor in profibrotic action of transforming growth factor-beta: A potential target for preventing renal fibrosis. Am J Kidney Dis 38 (4 Suppl 1): S134-S138, 2001.
25. Cao YL, Duan Y, Zhu LX, Zhan YN, Min SX and Jin AM: TGF-β1, in association with the increased expression of connective tissue growth factor, induce the hypertrophy of the ligamentum flavum through the p38 MAPK pathway. Int J Mol Med 38: 391-398, 2016.
26. Williams EJ, Gaça MD, Brigstock DR, Arthur MJ and Benyon RC: Increased expression of connective tissue growth factor in fibrotic human liver and in activated hepatic stellate cells. J Hepatol 32: 754-761, 2000.
27. Hopkins M, Tyson JJ and Novák B: Cell-cycle transitions: A common role for stoichiometric inhibitors. Mol Biol Cell 28: 3437-3446, 2017.
28. Jung KH, Kim JK, Noh JH, Eun JW, Bae HJ, Xie HJ, Ahn YM, Park WS, Lee JY and Nam SW: Targeted disruption of Nemo-like kinase inhibits tumor cell growth by simultaneous suppression of cyclin D1 and CDK2 in human hepatocellular carcinoma. J Cell Biochem 110: 686-696, 2010.
29. Meng L, Feng B, Tao H, Yang T, Meng Y, Zhu W and Huang C: A novel antiestrogen agent (3R,6R)-bassiatin inhibits cell proliferation and cell cycle progression by repressing Cyclin D1 expression in 17β-estradiol-treated MCF-7 cells. Cell Biol Int 35: 599-605, 2011.
30. Lange C, Huttner WB and Calegari F: Cdk4/CyclinD1 overexpression in neural stem cells shortens G1, delays neurogenesis, and promotes the generation and expansion of basal progenitors. Cell Stem Cell 5: 320-331, 2009.
31. Qin LF and Ng IO: Exogenous expression of p21 (WAF1/CIP1) exerts cell growth inhibition and enhances sensitivity to cisplatin in hepatoma cells. Cancer Lett 172: 7-15, 2001.
32. Cazzalini O, Perucca P, Riva F, Stivala LA, Bianchi L,Vannini V, Ducommun B and Prosperi E: p21CDKN1A does not interfere with loading of PCNA at DNA replication sites, but inhibits subsequent binding of DNA polymerase delta at the G1/S phase transition. Cell Cycle 2: 596-603, 2003.
33. Green DR: Apoptotic pathways: Paper wraps stone blunts scissors. Cell 102: 1-4, 2000.
34. Peng X, Yu Z, Liang N, Chi X, Li X, Jiang M, Fang J, Cui H, Lai W, Zhou Y and Zhou S: The mitochondrial and death receptor pathways involved in the thymocytes apoptosis induced by aflatoxin B1. Oncotarget 7: 12222-12234, 2016.
35. Kawada N: Human hepatic stellate cells are resistant to apoptosis: Implications for human fibrogenic liver disease. Gut 55: 1073-1074, 2006.
36. Novo E, Marra F, Zamara E, Valfrè di Bonzo L, Monitillo L, Cannito S, Petrai I, Mazzocca A, Bonacchi A, De Franco RS, *et al*: Overexpression of Bcl-2 by activated human hepatic stellate cells: Resistance to apoptosis as a mechanism of progressive hepatic fibrogenesis in humans. Gut 55: 1174-1182, 2006.
37. Saile B, Knittel T, Matthes N, Schott P and Ramadori G: CD95/CD95L-mediated apoptosis of the hepatic stellate cell. A mechanism terminating uncontrolled hepatic stellate cell proliferation during hepatic tissue repair. Am J Pathol 151: 1265-1272, 1997.
38. Tan C, Dlugosz PJ, Peng J, Zhang Z, Lapolla SM, Plafker SM, Andrews DW and Lin J: Auto-activation of the apoptosis protein Bax increases mitochondrial membrane permeability and is inhibited by Bcl-2. J Biol Chem 281: 14764-14775, 2006.
39. Bhowmick NA, Ghiassi M, Bakin A, Aakre M, Lundquist CA, Engel ME, Arteaga CL and Moses HL: Transforming growth factor-beta1 mediates epithelial to mesenchymal transdifferentiation through a RhoA-dependent mechanism. Mol Biol Cell 12: 27-36, 2001.
40. Wang Y, Ma J, Chen L, Xie XL and Jiang H: Inhibition of focal adhesion kinase on hepatic stellate-cell adhesion and migration. Am J Med Sci 353: 41-48, 2017.
41. Hinz B, Celetta G, Tomasek JJ, Gabbiani G and Chaponnier C: Alpha-smooth muscle actin expression upregulates fibroblast contractile activity. Mol Biol Cell 12: 2730-2741, 2001.